Influence of base course gradation on response of granular bases under cyclic loading: a micromechanical study

Influence au cours de la gradation de base, en reaction avec les bases granulaires sous chargement cyclique: une etude en micromechanique

J. Han, A. Bhandari & R.L. Parsons

The University of Kansas, United States of America.

ABSTRACT

Performance of unpaved granular bases relies on the shear strength and stiffness of granular particles. These two mechanical properties depend on shape, size, and gradation of the particles. This paper presents a micromechanical study on the influence of particle gradation on the response of unreinforced and geogrid-reinforced granular bases under cyclic loading. Commercial software, Particle Flow Code (PFC) 2D based on the discrete element method (DEM), was used for this purpose. Different biaxial assemblies of uniform particles and well-graded particles were sheared at low confining stresses for their stress-strain relationships and friction angles. The geogrid was simulated using one layer of bonded particles with different sizes to mimic its grid structures. Two base courses consisting of uniform particles and well-graded particles, which were subjected to a 5kN cyclic ramp load at a frequency of 0.76 Hz using a wheel, were modeled. The DEM study showed that the assembly of well-graded particles had a higher angle of internal friction than the assembly of uniform particles. Further, the addition of the geogrid reduced the deformation after each load cycle.

RÉSUMÉ

La performance des fondations granulaires non pavées est liée à la résistance au cisaillement et à la rigidité de ces composants granulaires. Ces deux propriétés mécaniques dépendent de la forme, de la taille, et de la granulométrie des particules. Cet article présente une étude « micromécanique » sur l'influence de la granulométrie sur la réponse des bases granulaires non renforcées et renforcées par un géotextile sous un chargement cyclique. Pour cette fin, le logiciel “Particle Flow Code (PFC) 2D”, basé sur la méthode aux éléments discrets (MED), a été utilisé. Différents combinaisons bi-axiales de particules à granulométrie étalée et uniforme ont été cisaillées à basse contrainte de confinement afin de déterminer la relation contrainte-déformation ainsi que les angles de frottement. Le géotextile a été simulé en utilisant une couche de particules liée ayant différentes tailles de grain afin de reproduire le plus possible son squelette. La modélisation s'est faite sur deux types de fondation granulaire (granulométrie étalée puis uniforme), qui ont été soumises à une charge de circulation cyclique de 5 kN à une fréquence de 0,76 hertz en simulant une roue. Les résultats issus de la MED ont montré que la matrice à granulométrie étalée possédait un angle de frottement interne plus élevé que celle à granulométrie uniforme. De plus, l'addition d'un géotextile réduisait la déformation après chaque cycle de chargement.

Keywords: Gradation, shear strength, geogrid, cyclic load, micromechanics

1 INTRODUCTION

Geosynthetics have been widely used since 1970s as a subgrade improvement or base reinforcement in the construction of unpaved roads (Giroud and Han, 2004). In the past, significant research has been done using experimental and numerical methods to study the interaction between geosynthetic and aggregate. Fannin and Sigurdsson (1996) and Hufenus et al. (2006) conducted full-scale field tests to investigate the benefits of geosynthetics on the reduction of rut depths of granular bases. Similarly, laboratory experiments using plate load tests have been done to evaluate the benefits of geosynthetics on minimizing the settlement and improving the bearing capcity under monotonic and cyclic loading conditions (Raymond and Ismail, 2003; Indraratna et al., 2007; Pokharel et al., 2009). Giroud and Han (2004) proposed a theoretically based and experimentally calibrated design method for geosynthetic-reinforced unpaved roads. Most studies consider the effects of granular bases using a single parameter. A classic example would be the use of California Bearing Ratio (CBR) value to characterize the base course, whereas its mechanical properties depend on gradation, shape, size, and mineralogical composition of the aggregate.

Satisfactory performance of unpaved roads (roads and rail tracks) depends primarily on the shear strength and stiffness of granular particles. Skermer and Hillis (1970) and Lekarp et al. (2000) found that the granular base with an optimal gradation could have the maximum shear strength and stiffness. Based on consolidated drained triaxial tests on four corse-grained (cohesionless) soils, Skermer and Hillis (1970) concluded that the gradation close to the Fuller curve yielded the maximum shear strength. The Fuller curve determines the size distribution of aggregates so as to provide the maximum density. However, Selig and Roner (1987) observed a constant shear strength of the coarse-grained soils tested at the same void ratio but with different gradations. The literature review by Selig and Roner (1987) and Lekarp et al. (2000) indicated contradictory findings regarding the influence of aggregate gradation on its shear strength and stiffness. This paper presents an analysis of the effect of gradation on the shear strength of aggregates and the responses of unreinforced and geogrid-reinforced unpaved bases under a cyclic wheel load using a discrete element method (DEM).

DEM modeling has been used to simulate different laboratory tests, including direct shear tests and triaxial tests. The DEM has also been used to investigate particle movement and contact forces between interacting particles under a cyclic load (Lobo-Guerrero and Vallejo, 2006; Saussine et al., 2006; Bhandari et al., 2009). These studies revealed how contact forces are transmitted in a granular medium under an applied load. In addition, the DEM is useful for examining the resilient behavior of the granular medium under a repeated load. In an attempt to explain the geogrid-aggregate interlocking in a particle level, Konietzky et al. (2004) modeled the triaxial tests of geogrid-reinforced samples in three dimensions using spheres. They noted that for aggregates with particle sizes from 0.6 to 20 mm, a punched-drawn biaxial geogrid had a confinement influence zone of 100 mm on either side of the geogrid. Subsequent studies by McDowell et al. (2006), using clumps to simulate the actual shape of aggregates, confirmed the extent of the confinement zone.

Proceedings of the 17th International Conference on Soil Mechanics and Geotechnical Engineering
M. Hamza et al. (Eds.)

doi:10.3233/978-1-60750-031-5-893

2 NUMERICAL MODELING

Particle Flow Code (PFC^{2D}), developed by Itasca based on the discrete element method (Itasca, 2004), was used in this study. PFC^{2D} is based on rigid body and soft contact approaches. The soft contact approach allows the calculations of the deformations at contacts.

The effect of aggregate gradation on its shear strength was first investigated in this study using biaxial simulation. The simulation also established the relationship between the micromechanical parameters and the macro-scale properties of the aggregate. Uniform sized particles of 10.3 mm in diameter as a baseline case, were generated in a rectangular box (401mm wide and 802mm high). The ratio of the width of the rectangular box to the diameter of the particles was 40, which is larger than that in the ASTM D 3080-04 standard but closely follows the recommendation of Jacobson et al. (2007) as a requirement to observe a shear band in a granular medium. The height of the rectangular box was twice its width. In the next biaxial simulation, different diameters of the particles were selected according to Fuller's curve. The distribution of the diameters of the particles was as follows: 19 mm - 25%, 12 mm - 25%, and 5 mm - 50%. The coefficient of uniformity ($C_u = D_{60}/D_{10}$) of the graded assembly was 2.4. It is worth mentioning that the weighted average of these three diameters corresponds to the diameter (10.3 mm) of the uniform particles used in the baseline case, however, their mean particle size (D_{50}) was 5mm, which is appropriately half the diameter of the uniform particles. Again, the ratio of the width of the box to the average diameter of the particles for the graded sample was maintained 40. Both samples had the same initial porosity of 0.16, which corresponds to a medium dense condition. Figure 1 shows the assembly of the generated particles. Micromechanical properties of soil particles are presented in Table 1. Three numerical tests were performed on each sample. The assembly was confined to an initial isotropic stress of 5, 10, and 15 kPa and then sheared at a low velocity of 6E-8 m/step. Such a low velocity ensured a quasi-static equilibrium at each stage of loading which was verified by monitoring the boundary work and the accumulated strain energy of the system. The computed stress-strain relationships will be presented and discussed in the next section.

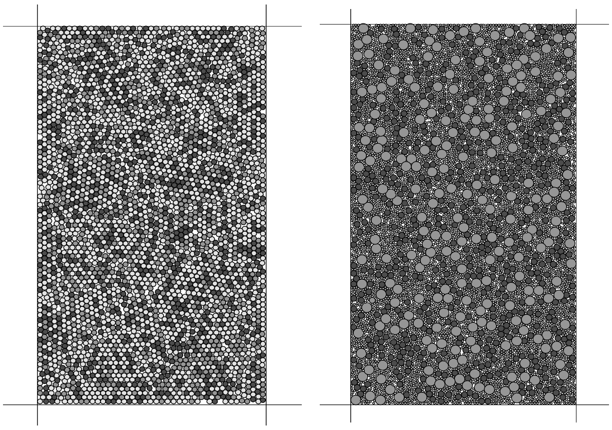

a) b)

Figure 1. Numerical sample preparation for biaxial simulation: a) single sized particles; b) different sized particles.

After determining the micromechanical parameters of the particles, an unpaved base section with a rigid subgrade was selected for simulation. The selection of the rigid subgrade was to eliminate the influence of the subgrade and focused on the response of the base course. A 1.25 m wide and 0.303 m high box was created by four walls. First, the box was divided into

Table 1. Micromechanical properties for DEM analysis.

Material	Parameters	
Soil	Shear stiffness of particles, k_s (MN/m)	75.0
	Normal stiffness of particles, k_n (MN/m)	62.5
	Friction coefficient (μ)	0.85
Geogrid	Shear stiffness of particles, k_s (MN/m)	645
	Normal stiffness of particles, k_n (MN/m)	645
	Friction coefficient (μ)	0.68
	Parameter of contact bond normal strength, ϕ_n (kN)	23.7
	Parameter of contact bond shear strength, ϕ_s (kN)	23.7
	Parallel bond normal stiffness, k_{np} (GN/m^3)	1290
	Parallel bond shear stiffness k_{sp} (GN/m^3)	1290
	Parallel bond normal strength, σ_{np} (MN/m^2)	95
	Parallel bond shear strength, σ_{sp} (MN/m^2)	95
	Parallel bond radius multiplier, r_{pb}	0.5

two compartments (below and above the geogrid) to ease the placement of the geogrid. The dimensions of the compartments were chosen so as to place the geogrid at the mid-depth of the base. Two numerical samples were prepared with the gradations of the particles same as those used in the biaxial simulation. The particles were generated simultaneously in both compartments. After the particles were generated, the assembly was cycled to meet the equilibrium of forces. It should be noted that the radius expansion technique generates large lateral forces on the wall, and hence the forces should be brought to an initial at-rest condition. Lateral walls were moved in opposite directions using the numerical servo mechanism until the desired lateral wall force (equal to the lateral earth thrust at the earth pressure coefficient of 1.0) was attained. The wall movement required to achieve the target wall forces was approximately 0.3% of the wall width in each direction and had a marginal effect on the porosity of the assembly. Figure 2 shows the numerical sample of graded particles.

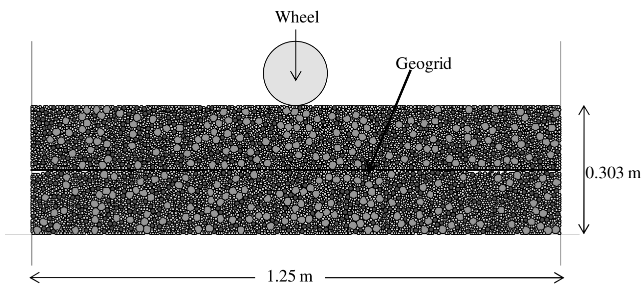

Figure 2. DEM model of a geogrid-reinforced graded base (19 mm - 25%, 12 mm - 25%, and 5 mm - 50%).

The geogrid was modeled using bonded particles of 1.0 mm diameter at ribs and 2.6 mm diameter at junctions. The center to center distance between the adjacent junctions was 30.6 mm, which is the aperture dimension in a cross machine direction for a selected punched-drawn biaxial geogrid. The contact bond force between the geogrid particles corresponds to its tensile strength (20 kN/m at 5% strain which is a linear portion of the tensile stiffness versus strain plot for the given geogrid). Similarly, the tensile stiffness of the geogrid corresponds to the normal stiffness between particles. The micromechanical parameters for the geogrid were calibrated by simulating a tensile strength test. The details of this calibration can be found in the previous research conducted by Bhandari et al. (2009). Table 1 presents the micromechanical parameters of the geogrid.

A cyclic ramp load, 5 kN in magnitude, was applied using a wheel of diameter 0.15 m and the resulted surface deformations were calculated. This load pulse had a 0.3 second period of linear load increase from 0 to 5 kN, followed by a 0.2 second period where the load was held at 5 kN, followed by a linear load decrease to 0 kN over 0.3 second period, then followed by 0.5 second period of 0 kN before the next loading cycle. It was applied in a vertical direction and had an equivalent frequency of 0.76 Hz. The responses of both unreinforced and geogrid-reinforced bases were investigated in this study. To minimize the effects of sample preparation on subsequent numerical results, the geogrid-reinforced base models were degraded into the unreinforced base models after deleting the particles that represented the geogrid. Though deleting the geogrid particles does not represent the field construction procedure, it is one of the viable options to ensure the use of same base course for reinforced and unreinforced cases in the numerical simulation.

3 RESULTS

Figures 3 and 4 show the relationship of stress and volumetric strain with axial strain at confining stresses of 5, 10, and 15 kPa for the assembly of uniform particles of 10.3 mm in diameter. Figures 5 and 6 show similar plots for the assembly of well-graded particles. Low confining stresses were selected to mimic typical stress levels in base courses. Both assemblies underwent negligible initial contraction followed by dilation during shearing. The assembly of uniform particles dilated more (max ε_v = 2%) than the assembly of graded particles (max ε_v= 1.5%). This phenomenon can be explained that small particles in well-graded particles can move into the gaps between large particles to minimize the dilation. Figures 3 and 5 show that the graded particles had slightly stiffer responses than the uniform particles. Figure 7 also illustrates a slight strength difference between these two assemblies. The angle of internal friction of the uniform assembly was 34.0^o ($\phi = \sin^{-1}$ (q/p')) while that of the graded assembly was 35.5^o. Even at the identical porosity (n=0.16), the graded assembly had a higher angle of internal friction than the uniform assembly. The improvement on the friction angle of the graded sample will be even larger if one considers the graded assembly at a low porosity as a result of ease in compaction.

Figure 8 shows the deformation of the base course with time when subjected to a cyclic ramp load. The numerical study was terminated once the deformation was beyond 100 mm since the acceptable rut depth of an unpaved road is 50-100 mm (Giroud and Han, 2004). Increase and decrease in the deformation correspond to the rising and falling ramps of the load cycle. It is shown that the unreinforced base of uniform particles only sustained the ramp load for two cycles before it had a deformation of 100 mm. On the other hand, the geogrid-reinforced base of uniform particles sustained the ramp load for eight cycles; therefore, the use of the geogrid increased the number of cycles by four times. Figure 8 also shows that the unreinforced graded base had better performance than the unreinforced base of uniform particles, which is consistent with the comparison of their shear strengths discussed before. However, the reinforced base of uniform particles outperformed the reinforced base of well-graded particles. This difference may result from different particle sizes since the size of the uniform particles is approximately twice the mean particle size (D_{50}) of the well-graded particles. The size of the uniform particles is approximately 1/3 the aperture size of the geogrid while the mean particle size of the graded particles is approximately 1/6 the aperture size of the size. The uniform particles with the larger particle size are more effective to interlock with the geogrid than the graded particles with the smaller mean particle size. Brown et al. (2006) found that the optimum geogrid aperture size was 65mm for a 50mm uniform aggregate. Further DEM analysis is needed for investigating the effect of the relative dimension of the particle size to the geogrid aperture size on the interlocking.

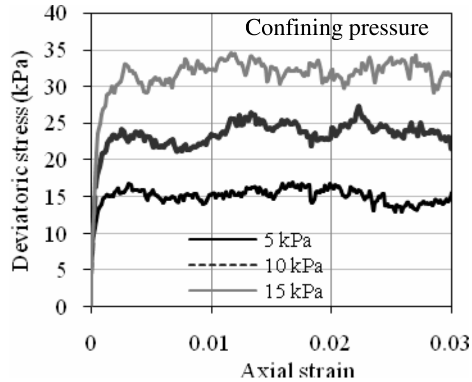

Figure 3. Stress-strain curve for uniformly graded particles of 10.3 mm diameter.

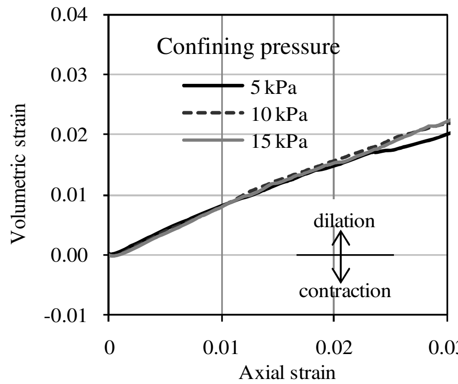

Figure 4. Volumetric strain vs axial strain for uniformly graded particles of 10.3 mm diameter.

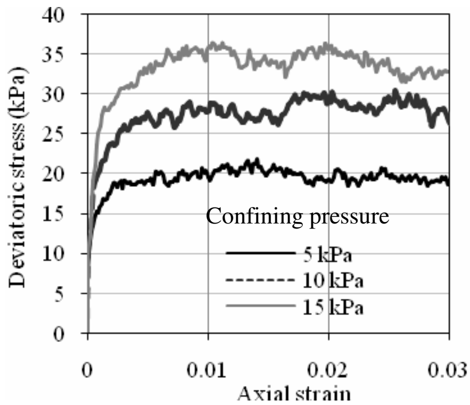

Figure 5. Stress-strain curve for well graded particles (19 mm - 25%, 12 mm - 25%, and 5 mm - 50%).

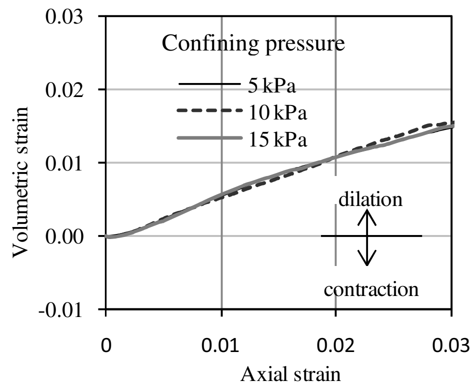

Figure 6. Volumetric strain vs. axial strain for well graded particles (19 mm - 25%, 12 mm - 25%, and 5 mm - 50%).

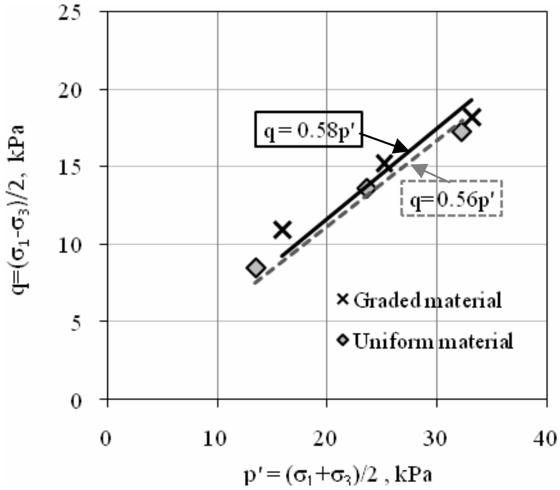

Figure **7.** q vs. p'.

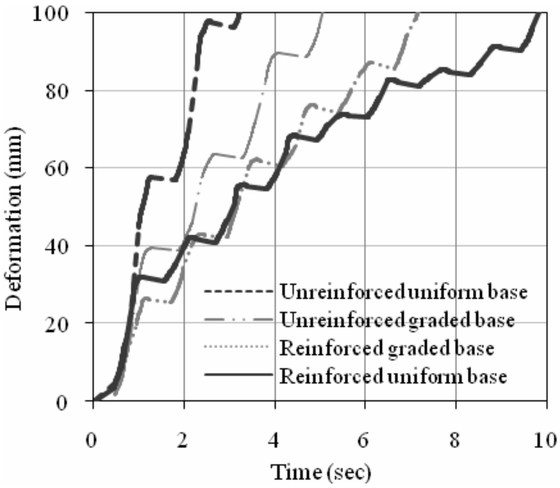

Figure 8. Deformation versus time.

4 CONCLUSIONS

This study investigated the effect of the particle gradation on the shear strength of the granular particles. Two-dimensional biaxial simulations of uniform sized particles and well graded particles showed that at an identical porosity (n = 0.16) and weighted average particle size, the assembly of well-graded particles had a slightly higher angle of internal friction than the assembly of uniform particles. An unreinforced base of well-graded particles performed better than that of uniform particles under cyclic loading. The geogrid reduced the deformation of the granular base. For the geogrid modeled in this study, the reinforced base of uniform particles outperformed the reinforced base of well-graded particles due to the better interlocking between the larger size of particles in the uniform particles.

REFERENCES

Bhandari, A., Han, J., Parsons, R.L., 2009. Discrete element method investigation of geogrid-aggregate interaction under a cyclic wheel load. CD-Rom publication, the *TRB 88th Annual Meeting*, January 11 to 15, Washington, DC.

Brown, S.F., Thom, N.H., and Kwan, J., 2006. Optimising the geogrid reinforcement of rail track ballast. *Railfound Conference*, Birmingham: 346-354.

Fannin, R.J., Sigurdsson, O., 1996. Field Observations on Stabilization of Unpaved Roads with Geosynthetics. *Journal of Geotechnical Engineering* 122 (7):544-553.

Giroud, J.P., Han, J., 2004. Design method for geogrid-reinforced unpaved roads. I. Development of design method. *Journal of Geotechnical and Geoenvironmental Engineering* 130 (8):775-786.

Hufenus, R., Rueegger, R., Banjac, R., Mayor, P., Springman, S.M., Bronnimann, R., 2006. Full-scale field tests on geosynthetic reinforced unpaved roads on soft subgrade. *Geotextiles and Geomembranes* 24 (1):21-37.

Indraratna, B., Shahin, M.A., Salim, W., 2007. Stabilisation of granular media and formation soil using geosynthetics with special reference to railway engineering. *Ground Improvement* 11 (1):27-43.

Itasca, 2004. *Paticle Flow Code in Two Dimensions*. Itasca Consulting Group, Inc., Minnesota.

Jacobson, D.E., Valdes, J.R., Evans, T.M., 2007. A numerical view into direct shear specimen size effects. *Geotechnical Testing Journal* 30 (6):1-5.

Konietzky, H., te Kamo, L., Groeger, T., Jenner, C., 2004. Use of DEM to model the interlocking effect of geogrids under static and cyclic loading. In *Numerical Modeling in Micromechanics via Particle Methods*, at Kyoto, Japan: 3-11.

Lekarp, F., Isacsson, U., Dawson, A., 2000. State of the art. I: resilient response of unbound aggregates. *Journal of Transportation Engineering* 126 (1):66-75.

Lobo-Guerrero, S., Vallejo, L.E., 2006. Discrete element method analysis of railtrack ballast degradation during cyclic loading. *Granular Matter* 8 (3-4):195-204.

McDowell, G.R., Harireche, O., Konietzky, H., Brown, S.F., Thom, N.H., 2006. Discrete element modelling of geogrid-reinforced aggregates. *Geotechnical Engineering* 159 (GEI):35-48.

Pokharel, S.K., Han, J., Leshchinsky, D., Parsons, R.L., and Halahmi, I., 2009. Experimental evaluation of influence factors for single geocell-reinforced sand. CD-Rom publication, the *TRB 88th Annual Meeting*, January 11 to 15, Washington, DC.

Raymond, G., Ismail, I., 2003. The effect of geogrid reinforcement on unbound aggregates. *Geotextiles & Geomembranes* 21 (6):355.

Saussine, G., Cholet, C., Gautier, P.E., Dubois, F., Bohatier, C., Moreau, J.J., 2006. Modelling ballast behaviour under dynamic loading. Part 1: A 2D polygonal discrete element method approach. *Computer Methods in Applied Mechanics and Engineering* 195 (19-22):2841-2859.

Selig, E.T., Roner, C.J., 1987. Effects of particle characteristics on behavior of granular material. *Transportation Research Record* (1131):1-6.

Skermer, N.A., Hillis, S.F., 1970. Gradation and shear characteristics of four cohesionless soils. *Canadian Geotechnical Journal* 7 (1):62-8.